Simulated Variability of the Arctic Ocean Freshwater Balance 1948–2001

CORNELIA KÖBERLE AND RÜDIGER GERDES

Alfred-Wegener-Institut für Polar- und Meeresforschung, Bremerhaven, Germany

(Manuscript received 1 May 2006, in final form 4 August 2006)

ABSTRACT

The Arctic Ocean freshwater balance over the period 1948–2001 is examined using results from a hindcast simulation with an ocean–sea ice model of the Atlantic and Arctic Oceans. Atmospheric forcing is taken from the NCEP–NCAR reanalysis and different terrestrial freshwater sources as well as the Bering Strait throughflow are specified as constant seasonal cycles. The long-term variability of the Arctic Ocean liquid freshwater content is determined by the variability of lateral exchanges with the subpolar seas. Surface freshwater flux variability is dominated by the thermodynamic growth of sea ice. This component of the freshwater balance has larger variability at interannual frequencies. The Arctic Ocean liquid freshwater content was at a maximum in the middle of the 1960s. Extremely low liquid freshwater export through Fram Strait caused this maximum in the freshwater content. The low export rate was related to weak volume transports in the East Greenland Current. Low volume transports were forced by a reduction in sea surface height across Fram Strait, triggered by anomalous meltwater from Barents Sea ice export that was carried toward Fram Strait with the West Spitzbergen Current. After the 1960s maximum liquid freshwater content, the Arctic Ocean gradually returned to an equilibrium between export through the passages toward the Atlantic and the freshwater sources.

1. Introduction

Relative to its surface area, the Arctic Ocean collects and stores a disproportionate amount of freshwater, mostly from runoff from the Siberian rivers that drain a large land surface area. Atlantic Ocean water flowing into the Arctic Ocean via the Barents Sea and Fram Strait is transformed into colder and fresher water that forms part of the return Atlantic water. Return Atlantic water is carried with the East Greenland Current (EGC) toward Denmark Strait. This water is an important component of Denmark Strait Overflow Water (DSOW) and also contributes to the Faeroe–Scotland overflow, the precursors of lower North Atlantic Deep Water (Mauritzen 1996). The upper parts of the EGC carry sea ice and relatively fresh water of Arctic Ocean origin toward lower latitudes where this freshwater can affect deep-water production. The freshwater reservoirs of the Arctic Ocean, the freshwater above the Arctic halocline, and the sea ice can buffer fluctuations in the freshwater sources. On the other hand, they can also feed freshwater export events that constitute large climate anomalies in the downstream ocean basins (Dickson et al. 1988).

Exchanges with the Atlantic couple the Arctic to the global oceanic circulation. The Nordic seas have freshened in recent decades leading to reduced overflow through the Faroe–Shetland Channel (Hansen et al. 2001). Dickson et al. (2002) document a freshening of the deep layers of the northern North Atlantic along the pathways of the overflow water masses. Curry and Mauritzen (2005) quantify the dilution of the Nordic seas and the subpolar North Atlantic as an addition of $19\,000 \pm 5000$ km^3 between 1965 and 1995 with more than one-half of the total freshwater added within five years at the end of the 1960s. A redistribution of freshwater within the Arctic is a possible cause for the observed freshening of the Nordic seas and the subpolar North Atlantic.

Coincident with the freshening of the subpolar North Atlantic and the Nordic seas, the Arctic sea ice volume has decreased over the last three to four decades. Rothrock et al. (1999) report a decrease of the Arctic ice volume by about 40% between the mid-1960s and mid-1990s. Other authors observe a similar long-term decrease in sea ice thickness (Wadhams and Davis 2000;

Corresponding author address: Cornelia Köberle, Alfred-Wegener-Institut, Bussestr. 24, 27570 Bremerhaven, Germany.
E-mail: ckoeberl@awi-bremerhaven.de

DOI: 10.1175/JPO3063.1

Tucker et al. 2001) that has also been confirmed in model simulations (Holloway and Sou 2002; Köberle and Gerdes 2003; Zhang et al. 2000). Model experiments (Köberle and Gerdes 2003) indicate that reduced formation of sea ice caused this decrease. Sea ice export, on the other hand, did not increase over the last 50 years according to these simulations and the estimates based on a statistical relationship between ice transport and the sea level pressure (SLP) difference across Fram Strait by Vinje (2001). Thus, sea ice cannot directly be responsible for the freshening of the subarctic seas.

Little is known about the variability of the Arctic liquid freshwater reservoir and the oceanic exchanges with the subarctic seas. Aagaard and Carmack (1989) describe the mean Arctic freshwater budget for conditions until the 1980s, while Carmack (2000) provides a recent overview. The available historic salinity data for the Arctic Ocean is insufficient to fully assess the variability of the freshwater content over the last 50 years. Swift et al. (2005) reanalyzed the Timokhov and Tanis (1997, 1998) dataset and found that the upper Arctic Ocean was saltier during the last two decades than during the previous period covered by the data. The salinity anomaly appeared in the late 1970s both in the Eurasian and Canadian Basins. This widespread and early salinification has thus to be distinguished from the diversion of river water in the 1990s from the Eurasian Basin, the so-called retreat of the Arctic halocline (Steele and Boyd 1998).

Here, we assess the Arctic liquid freshwater balance in a version of the North Atlantic–Arctic Ocean Sea Ice Model (NAOSIM) hierarchy of the Alfred Wegener Institute over the last 50 years. After a short description of model components and forcing data (section 2), we consider the climatological freshwater balance in the model over the integration period (section 3). Section 4 describes the variability of the freshwater balance, while we discuss the mechanisms that force this variability in section 5. Summary and conclusions are provided in section 6.

2. Model description

The simulations were performed with a coupled ocean–sea ice model that was forced by prescribed surface wind stresses and by surface heat and salt fluxes that are calculated using given atmospheric fields and calculated SST and sea ice thickness and concentration. Köberle and Gerdes (2003, hereinafter KG03) used the model in a similar setup to investigate the Arctic sea ice volume variability.

a. Ocean model

The ocean model derives from the Geophysical Fluid Dynamics Laboratory Modular Ocean Model (MOM-2: Pacanowski 1995). It solves the primitive equations for the horizontal velocity components, temperature, and salinity. Vertical velocity, density, and pressure are calculated from diagnostic equations. The advection of tracers is handled by the flux-corrected transport scheme (Zalesak 1979; Gerdes et al. 1991), which is distinguished by its low implicit diffusion while still avoiding false extrema ("overshooting") in advected quantities. The implicit diffusion associated with the advection scheme is the only diffusion acting on the tracers in these experiments. Friction is implemented as Laplacian diffusion of momentum with horizontal and vertical viscosities of $A_{\mathrm{MH}} = 2.5 \times 10^4\ \mathrm{m^2\ s^{-1}}$ and $A_{\mathrm{MV}} = 10^{-3}\ \mathrm{m^2\ s^{-1}}$, respectively. The model domain encompasses the Atlantic north of approximately 20°S, including the entire Arctic Ocean. Open boundary conditions following Stevens (1991) have been implemented at the southern boundary and at Bering Strait. Monthly mean values for the streamfunction of the vertically integrated flow for the southern boundary have been taken from the Family of Linked Atlantic Model Experiments (FLAME) model of Kiel University (C. Dieterich 2001, personal communication), while temperatures and salinities at inflow points are taken from climatology. The monthly varying values for the transport through Bering Strait have been taken from Roach et al. (1995) and are distributed linearly over the three-gridpoint-wide strait. In comparison with the recent assessment of Woodgate and Aagaard (2005), these numbers are about 800 $\mathrm{km^3\ yr^{-1}}$ too small because they neglect the influx of the Alaskan Coastal Current and the import of sea ice through Bering Strait. Linear interpolation to the time step of the model is done for all time-varying input fields.

To avoid the singularity of geographical spherical coordinates at the pole the model is formulated on a rotated spherical grid where the equator coincides with the geographical 30°W meridian. The pole of this grid lies at 60°E on the geographical equator. The horizontal resolution is $1^\circ \times 1^\circ$ in the rotated grid, resulting in nearly equal spacing of about 100 km in both horizontal directions in the entire Arctic Ocean. In the vertical, the model contains 19 unevenly spaced levels. Bottom topography is derived by horizontal averaging of the 5-Minute Gridded Elevation Data (ETOPO5) dataset of the National Geophysical Data Center (1988). Modifications were made in Denmark Strait and the Faroe Bank Channel area to retain the sill depths of the passages. Grid points are regarded as land when more than

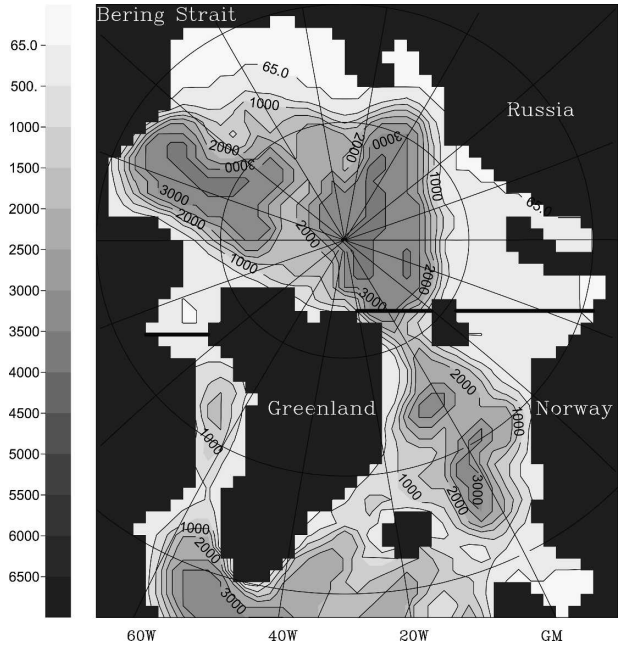

FIG. 1. Part of the model domain with bottom topography [depth (m)] and names of features mentioned in the text. Integral quantities for the Arctic Ocean have been integrated within the area outlined by thick black lines. Arctic freshwater export was calculated across these boundaries.

40% of the original ETOPO5 data points within a grid box are land. The Canadian Archipelago is opened by increasing the requirement to 80% land points within the grid box. Thus, a passage of at least two active tracer boxes wide is introduced that connects the Canadian Basin with Baffin Bay (Fig. 1).

b. Sea ice model

The ocean model is coupled with a dynamic–thermodynamic sea ice model that has been developed by Harder (1996) from the original Hibler (1979) model. The prognostic variables are sea ice and snow thickness, ice concentration, and ice age, while sea ice drift is diagnosed from the momentum balance where explicit time dependence has been neglected. This model has been used as a stand-alone model in otherwise identical configuration and identical parameters in the Sea Ice Model Intercomparison Project (SIMIP; Lemke et al. 1997; Kreyscher et al. 2000).

c. Coupling of ocean and sea ice components

Sea ice and ocean models use the same time step and the same horizontal grid except for the southern boundary of the ice model located at approximately 50°N. Flow of ice out of the domain is allowed at the southern boundary and at Bering Strait. Ice advected across these boundaries vanishes immediately, with no freshwater being transferred to the ocean. Ice transport across the southern boundary was monitored and remained negligible during the whole integration. The models are coupled following the procedure devised by Hibler and Bryan (1987). The sea ice is forced by wind stress, internal ice stress, a quadratic ocean–ice drag, Coriolis force, and surface tilt. The latter is estimated from the ocean velocities at 30-m depth that are assumed to be in geostrophic balance. The sea ice component calculates the surface heat fluxes from standard bulk formulas using prescribed atmospheric data and SST predicted by the ocean model.

d. Initial data and atmospheric forcing

Ice and ocean start from rest. Annual mean potential temperatures and salinities in the ocean were taken from the Polar Science Center Hydrographic Climatology (Steele et al. 2001a). Ice concentration, ice thickness, and snow thickness were initialized with the result of a previous experiment to avoid "shocking" the ocean with an initially large freshwater flux owing to excessive ice melting or freezing in response to its adjustment to the atmospheric forcing (see KG03 for details).

Forcing data are derived from the National Centers for Environmental Prediction–National Center for Atmospheric Research (NCEP–NCAR) reanalysis dataset 1948–2003 (see information online at http://www.cdc.nooa.gov). We use daily wind stress, surface (2 m) air temperature, and scalar wind. Relative humidity is set to 0.9 north of 60°N while an annual mean climatology from the NCEP–NCAR data is used south of 60°N. Surface freshwater fluxes are due to melting and freezing of snow and sea ice. A climatological annual cycle for precipitation is taken from Xie and Arkin (1996) while cloud cover is taken from Röske (2006). Evaporation is calculated using a bulk formula (Parkinson and Washington 1979). Continental runoff is included as the flow of 20 major rivers according to a climatological annual cycle derived from data of the Global Runoff Data Center (Table 1). The flow of Arctic rivers is augmented by 700 $km^3\ yr^{-1}$ to account for diffuse (nongauged) runoff (Prange and Gerdes 2006). The model also receives freshwater from the Baltic Sea, Hudson Bay, and Norwegian coastal runoff. The freshwater flows are transformed into a salt flux by multiplying with the local surface salinity at the river mouth. Total salinity is thus not conserved, a consideration that is of lesser concern in our regional model than the drawbacks involved in the alternative use of a constant reference salinity. With the local salinity we achieve higher accuracy and avoid possible reduction of the lo-

TABLE 1. Annual mean freshwater runoff into the Arctic Ocean implemented in the model following the AOMIP protocol (information online at http://fish.cims.nyu.edu/project_aomip/overview.html). Arctic river runoff is enhanced by a factor of 1.3 to account for ungauged runoff. The model also includes major subarctic rivers and contributions from Norwegian coastal runoff (247 km^3 yr^{-1}), Hudson Bay outflow (462 km^3 yr^{-1}), and Baltic Sea outflow (628 km^3 yr^{-1}).

Source	Annual mean runoff
Pechora	192
Ob + Pur	553
Yenisey	740
Olenek	41
Yana	42
Indigirka	66
Kolyma	128
Mackenzie	375
Severnaya Dvina	137
Lena	682
Khatanga	86
Taimyra	46
Pyasina	112

cal salinity below zero. It should be noted that the present rigid-lid model does not take into account the changes in sea level associated with volume flux through the surface or lateral boundaries.

e. Experimental procedure

The model was started from initial conditions and integrated with the variable forcing for four periods ($4 \times 54 = 216$ yr) of the NCEP–NCAR reanalysis forcing. During this spinup, surface salinity was restored toward prescribed surface salinity. The time constant for the restoring is 180 days. The reference salinities are climatological annual mean data from Steele et al. (2001a). Although used in many studies of Arctic Ocean circulation (Steele et al. 2001b), surface salinity restoring is not adequate in a study of the freshwater balance of the Arctic Ocean. The strong temporal variability of the restoring term under variable atmospheric forcing especially makes the interpretation of the results difficult. Thus, the model was reinitialized with the result from the end of the third cycle of NCEP–NCAR forcing (beginning of year 163 of the integration). For the repetition of the fourth forcing cycle, the restoring of surface salinities was switched off. However, without forcing toward climatology the model will drift away from reasonable distributions within the final 54 years of the integration because of model biases and the prescribed fluxes that are not adjusted to provide a closed freshwater balance.

To avoid this model drift, the surface salinity restoring term was analyzed over the fourth cycle of the atmospheric forcing and an annual mean climatology of that term was calculated. The annual mean climatology of the restoring term was applied as a fixed salt flux to the surface box of the ocean model in the final repetition of the fourth cycle of the atmospheric forcing.

3. Climatological freshwater balance

Ocean (e.g., Gerdes and Schauer 1997) and ice model (Lemke et al. 1997; Kreyscher et al. 2000; Hilmer 2001) components have been validated in stand-alone mode. KG03 discuss the simulation of Arctic sea ice in the coupled model. For the coupled system in this paper we concentrate on the climatological liquid freshwater content of the Arctic Ocean and the time-mean components of the freshwater balance.

a. Freshwater content climatology

The interior Arctic is characterized by a strong pycnocline that is due to a strong salinity stratification in the upper 200 m. The excess of freshwater relative to a column with mean salinity 35 psu is used to quantify the strength of the halocline in Fig. 2. For a discussion of the proper reference salinity for the Arctic Ocean freshwater balance see Prange and Gerdes (2006). Climatological data include negative values associated with the higher salinity of the Atlantic water in the Barents Sea and north of the Barents and Kara Seas. The Bering Strait inflow of Pacific Ocean water is also a source of relatively saline water for the ambient water in the western Arctic, although salinities are clearly below the reference value. A maximum, ~20 m, freshwater column is located in the central Beaufort Sea. The front between fresh and saline water masses approximately marks the transpolar drift from the East Siberian Sea to Fram Strait. Considerable freshwater storage is also noticeable in the Laptev and East Siberian Seas.

The model result exhibits similar features that also favorably compare quantitatively with the observed climatology. The influence of the Atlantic water in the eastern Arctic is somewhat less pronounced, especially north of the Barents Sea. The maximum freshwater column in the central Arctic exceeds the climatological values and is shifted westward. North of Greenland, the model shows a relatively constant freshwater column height, whereas the climatology features eastward declining freshwater content. Discrepancies also exist in the Laptev and Kara Seas where the model stores more freshwater than observed. These areas receive river runoff from the Ob, Yenisey, and Lena Rivers, the largest rivers in the Eurasian Arctic. As will be explained below in section 3c, the model is not able to efficiently

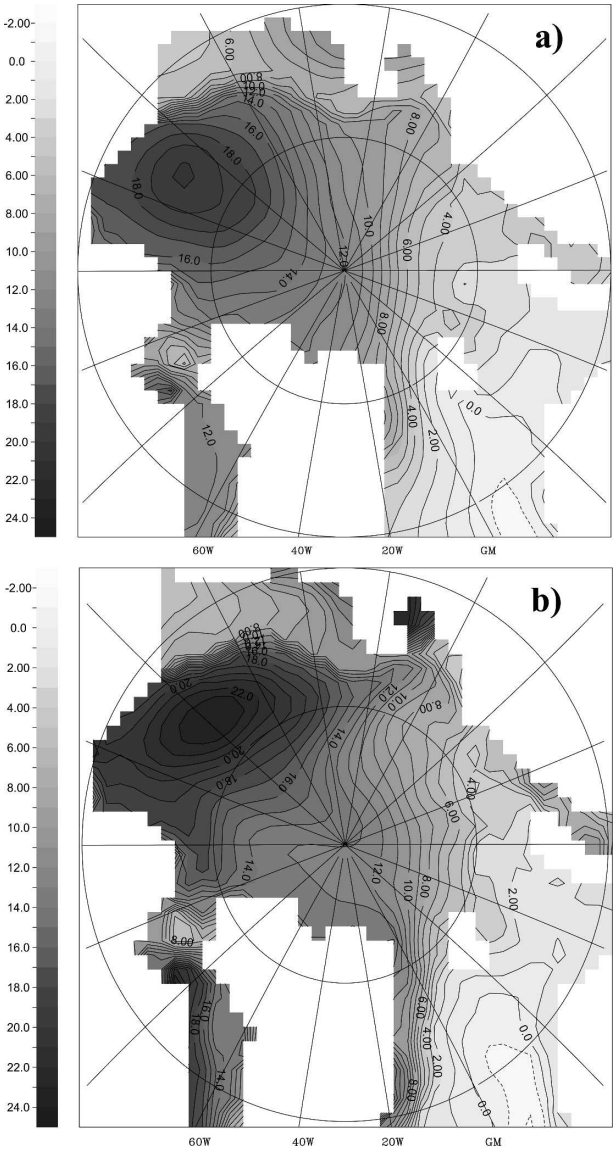

FIG. 2. Freshwater content, measured as the thickness of a column of freshwater to be added to a water column of constant 35-psu salinity to arrive at the observed salinity. Derived from (a) the PHC atlas (Steele et al. 2001a) and from (b) the model result averaged over the last 54 years of the simulation.

move the river water from the rather enclosed shelf seas into the interior of the Arctic.

b. Sources and sinks of Arctic freshwater

The freshwater content is not indicative of the freshwater dynamics. For that purpose, we compare freshwater fluxes across the boundaries of the domain with those compiled by Aagaard and Carmack (1989) in Table 2. The Arctic receives freshwater (reference salinity 35.0 psu) mainly through runoff, Bering Strait, and precipitation minus evaporation ($P - E$). The largest freshwater sinks are the transports through Fram Strait, the Canadian Archipelago, and the formation of sea ice. The formation of sea ice balances the ice export through Fram Strait (3306 km^3 yr^{-1}), the Barents Sea (1016 km^3 yr^{-1}), and the Canadian Archipelago (314 km^3 yr^{-1}). The ice transport through Fram Strait is in reasonable agreement with other estimates, for example, the 2900 km^3 yr^{-1} by Vinje (2001). A factor that somewhat distorts the comparison between observational estimates and model results is our choice of boundary for the Arctic Ocean (Fig. 1). The ice export through the Barents Sea is 1016 km^3 yr^{-1} in the model. Almost all of this ice melts within the geographical region of the Barents Sea and thus represents an artificial freshwater sink for the Arctic Ocean (including the Barents Sea). A more detailed validation of the model's sea ice component can be found in KG03.

Relative to Aagaard and Carmack (1989), the model underestimates the runoff, a consequence of given volume flux rates and the transformation into an equivalent salt flux using the local surface salinity. The local surface salinity near the major rivers is significantly smaller than the reference salinity that is then used to compute the terms in the freshwater balance. A newer estimate of the continental runoff by Shiklomanov et al. (2000) (4300 km^3 yr^{-1}) implies an even bigger model deficit in freshwater supply to the Arctic Ocean. Furthermore, the model probably overestimates the losses through Fram Strait and the Canadian Archipelago. Overall, the largest discrepancies between model and observational estimates are due to the liquid freshwater transport through Fram Strait, continental runoff, and too small freshwater influx through Bering Strait (see section 2).

Clearly, the freshwater balance exhibits some shortcomings of the model. For instance, to allow for a transport through the Canadian Archipelago, the opening between the Arctic and Baffin Bay had to be made exceedingly broad. This could well be a reason for an overestimate of that freshwater transport. It should be noted, however, that estimates of the freshwater transport through the Canadian Archipelago are very difficult to achieve (see Melling 2000), and thus vary widely. With a reference salinity of 34.8 psu, Steele et al. (1996) arrive at a value of 1230 km^3 yr^{-1}, while their estimate for liquid freshwater export through Fram Strait is only 756 km^3 yr^{-1}. Recently, Prinsenberg and Hamilton (2004) estimated 1418 $\pm$ 473 km^3 yr^{-1} for the western Lancaster Sound from mooring data taken between August 1998 and August 2001, also with a reference salinity of 34.8 psu. According to these authors, the total liquid freshwater transport through the Canadian

TABLE 2. Long-term annual mean contributions to the Arctic liquid freshwater balance ($km^3\ yr^{-1}$). Observational estimates are taken from Aagaard and Carmack (1989), recalculated for a reference salinity of 35 psu and a sea ice salinity of 3 psu. The net meltwater flux is taken as equal to the combined sea ice export rates (2880 $km^3\ yr^{-1}$ through Fram Strait and 140 $km^3\ yr^{-1}$ through the Canadian Archipelago) from Aagaard and Carmack (1989). Model figures are averages over the last 50 years of the simulation. Positive values indicate a freshwater source for the Arctic.

	Bering Strait	Canadian Archipelago	Fram Strait	BSO	$P - E$	Runoff	Net meltwater	Flux adjustment	Sum
Observational estimate	1800	−1220	−1330	270	900	3300	−3020	—	700
Model	1922	−2259	−3001	289	1576	2404	−4087	3078	−78
Difference	−122	1039	1671	−19	−676	896	1067	—	
Standard deviation	29	572	905	276	135	38	845	0	

Archipelago amounted to ~3000 $km^3\ yr^{-1}$ during the period of measurements.

Recalculated for a reference salinity of 35.0 psu, the values for freshwater transport are as follows: Fram Strait 855 $km^3\ yr^{-1}$ and the Canadian Archipelago 1318 $km^3\ yr^{-1}$ (Steele et al.) and Lancaster Sound 1546 ± 515 $km^3\ yr^{-1}$ and the Canadian Archipelago 3600 $km^3\ yr^{-1}$ (Prinsenberg and Hamilton).

Estimates of liquid freshwater transport through Fram Strait vary from Aagaard and Carmack's (1989) 1330 $km^3\ yr^{-1}$ to values of 2000–3700 $km^3\ yr^{-1}$ (Meredith et al. 2001). Meredith et al. base their estimates on observations of $\delta^{18}O$, salinity, and velocity at 79°N during August–September 1997 and 1998.

From this short discussion, we conclude that the ranges of individual observational estimates for lateral fluxes in the Arctic freshwater balance include our model values in most cases or come reasonably close to the model values. Still, there is the need for a flux adjustment in the model that is of equal magnitude to the largest individual components of the freshwater balance.

c. Surface freshwater flux adjustment

The spatial distribution of the freshwater flux owing to the flux adjustment is shown in Fig. 3. It exhibits largest positive values, indicating a freshwater source for the ocean model, over the Siberian shelf seas and in a tongue extending from the Laptev and Kara Seas toward the North Pole. The spatial structure suggests that the flux mainly compensates for a lack of freshwater originating from the Siberian rivers and following the transpolar drift into the interior Arctic. Runoff in the model is around 1000–2000 $km^3\ yr^{-1}$ less than more recent estimates (Shiklomanov et al. 2000). More important, however, is the failure of the model to disperse the freshwater away from the coasts. The insufficient communication between shallow shelf seas and the deep interior is a common problem in this class of ocean models. River water accumulates near the river mouths, leading to unrealistically low salinities. This diminishes the efficiency of the freshwater flux that is transformed into a salt flux by multiplying with the local surface salinity. While this is a more accurate procedure than using a constant reference salinity, the corresponding changes in ocean volume are neglected in the rigid-lid model (Prange and Gerdes 2006). However, free surface models also suffer from insufficient dispersion of freshwater from the coast (e.g., Griffies et al. 2005).

In other areas of the Arctic, the flux adjustment is typically less than 0.5 m yr^{-1} in each direction. These values still are comparable to the annual mean precipitation in this area.

We cannot exclude, however, that these fluxes partly compensate for a mismatch between the climatological surface salinities, based on observations mainly between 1950 and 1990, and the forcing period that ex-

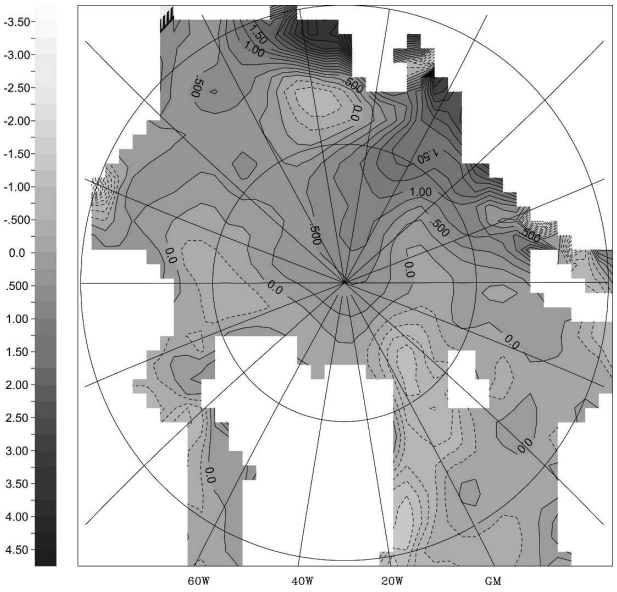

FIG. 3. Surface freshwater flux (m yr^{-1}) that is used as a flux adjustment. Positive values represent a freshwater flux into the ocean.

tends to 2001. For instance, north of the strong freshwater input through the flux adjustment we find an area where freshwater is extracted. This can be ascribed to the changed pathways of river water in times of the strongly positive North Atlantic Oscillation (NAO) toward the end of the twentieth century (Steele and Boyd 1998) that is not well represented in the climatological surface salinities. Similarly, the climatology might not reflect completely the supposed high ice export rates from the Arctic during positive NAO phases, thus featuring relatively low surface salinities in the sea ice formation regions and relatively high salinities in the melting regions of the EGC. In the Greenland Sea, it can furthermore be argued that the climatological salinity field is too smooth and low salinities extend too far into the interior of the Nordic seas. The model's more realistic EGC is comparatively narrow and restricted to the shelf and shelf break.

4. Variability of the Arctic freshwater balance

a. Freshwater content changes

The behavior of the model over the spinup period (years 0–162) and under the two different surface conditions (years 163–216) for salinity is illustrated in Fig. 4, which shows the time series of freshwater content (relative to a water column of constant salinity of 35 psu) integrated over the upper 350 m of the Arctic. The freshwater content increases slightly over the spinup period and levels off at the end of the integration period. The pattern of decadal to multidecadal variability repeats itself within each subperiod of 54-yr duration (Fig. 4a). Each subperiod, however, starts with different initial conditions as the forcing of the late 1940s follows the forcing of the early years of the current century. This mismatch between the forcing and the previous development of the ocean state leads to a new adjustment at the beginning of each subperiod of the ocean circulation and hydrography that lasts for approximately 15 yr, the time scale of water mass renewal in the Arctic Ocean halocline and Atlantic water layer. Despite these adjustments there are certain robust features that reoccur in each subperiod (Fig. 4c).

Comparing the results with the interactive restoring and the flux adjustment with a constant flux derived from the restoring over the last subperiod (Fig. 4b), we find a similar temporal variability in Arctic Ocean freshwater content. However, the amplitude of the long-term variability is enhanced. The freshwater content is systematically higher in the flux-adjusted case, but the value at the end of the integration is close to that of the restored case again, indicating that no substantial shift in the circulation regime has occurred due to the change in the surface boundary conditions. We conclude that the model does not suffer from the tendency toward unrealistically high sensitivity of the large-scale oceanic circulation under mixed boundary conditions (Zhang et al. 1993; Rahmstorf and Willebrand 1995; Lohmann et al. 1996).

With the flux adjustment there is no damping of salinity anomalies toward climatology, although there is still an artificial salt source to compensate for deficiencies in the model and the freshwater flux data. Surface salinity shows larger variability than with restoring because anomalies are not artificially damped. While we expect higher variability without the negative feedback of restoring, it is perhaps surprising that the mean Arctic freshwater content differs largely between the two surface boundary cases. Restorating removes freshwater from the Arctic in the early phase of the reanalysis period since salinity tends to be low as a consequence of relatively little liquid freshwater export and ice export from the Arctic. The opposite is true for the remainder of the integration. The constant flux adjustment allows the accumulation of freshwater as a consequence of reduced exports and does not provide additional freshwater after 1970 when freshwater is again exported in larger quantities from the Arctic.

Averaged over the period of then-available NCEP–NCAR atmospheric forcing data, the freshwater content integrated over the Arctic is around 10^5 km^3 in the simulation, slightly higher than the estimate of Aagaard and Carmack (1989) or the value diagnosed from the climatological Polar Science Center Hydrographic Climatology (PHC) dataset (84 000 km^3). Maximum freshwater content is reached in the late 1960s, followed by a decline that persists until the end of the integration. Decadal variability with minimum freshwater content around 1977, 1986, and 1997 is superimposed on the decreasing trend. The freshwater content time series has thus some similarity with the temporal development of the sea ice volume in the Arctic as calculated by KG03. Sea ice volume decreases from a pronounced mid-1960s maximum. Minima of sea ice volume occur around 1985 and 1995 with a lesser minimum in the mid-1970s. The parallel development of liquid freshwater content and sea ice volume already indicates that the changes in sea ice cannot be responsible for the long-term changes in the liquid freshwater content. The decline in both reservoirs after their maximum in the late 1960s might, instead, be due to one common cause.

b. Variability of sources and sinks

To characterize the variability of the different contributors to the Arctic freshwater balance we have listed in Table 2 the standard deviation of the annual

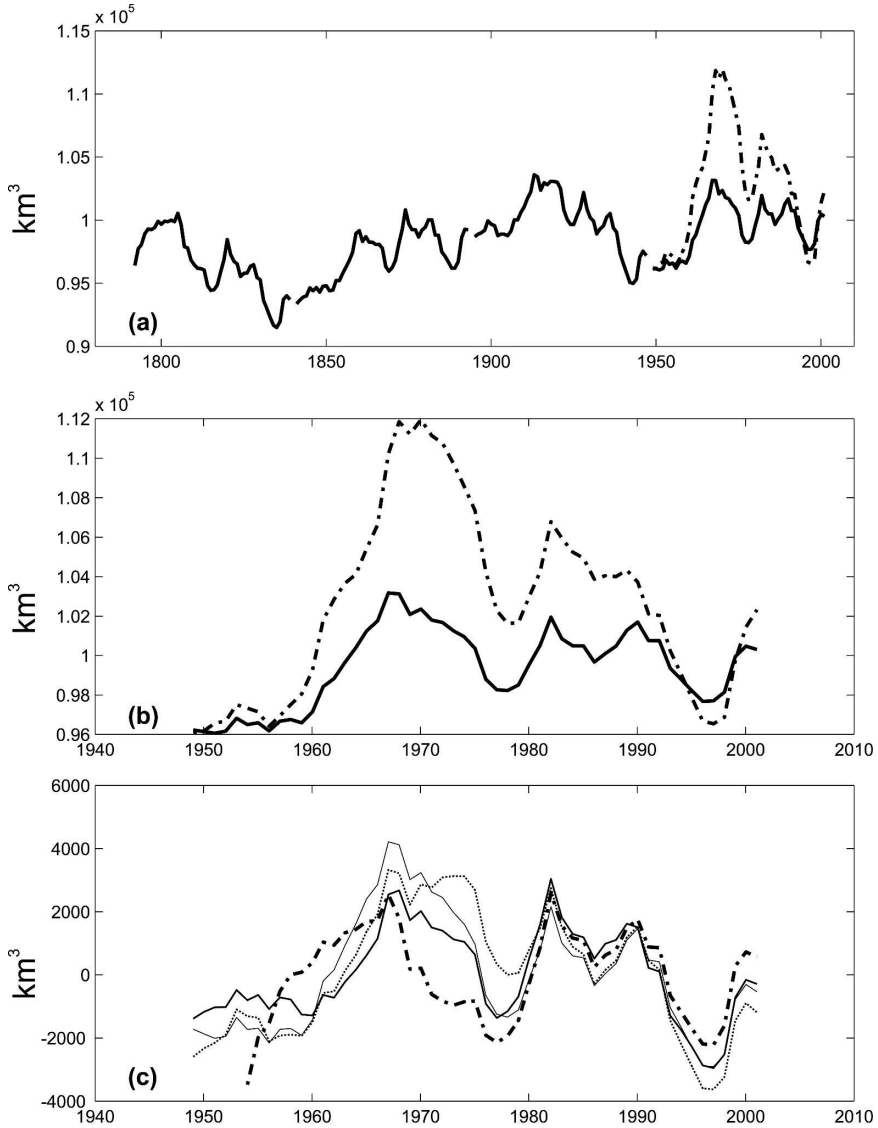

FIG. 4. (a) Time series of the freshwater content in the upper 350 m of the Arctic Ocean. For boundaries see Fig. 1. The integration lasts for 216 yr, i.e., four repetitions of the NCEP–NCAR forcing period 1948–2001. The time axis from 1783 thus does not imply atmospheric forcing from that period. The last NCEP–NCAR period has been repeated with the constant flux adjustment of Fig. 3 replacing the surface salinity restoring (dash–dotted line). (b) The last repetition of the NCEP–NCAR forcing is shown in more detail. (c) The detrended time series for each 54-yr subperiod (dash–dotted: first cycle; thick solid: second cycle; dotted: third cycle; thin solid: last cycle) of the integration show similar decadal to multidecadal variability.

means. According to this metric, the Fram Strait transport and thermodynamic ice growth contribute the most to the variability of the freshwater fluxes that enter the system. The components of the surface flux are shown in Fig. 5 and the contributions of the different lateral transports are given in Fig. 6.

Although precipitation is a prescribed constant surface freshwater flux, the amount that enters the ocean is actually variable because this part is strongly modified by the ice cover. Much of the precipitation is stored as snow on sea ice and is released later under melting conditions. Since ice cover changes interannually, the amount of snow varies. Evaporation also depends on the area of open water. Still, the variability is rather minor, so Bering Strait transport and net precipitation will not be considered in the following. Runoff is a constant freshwater flux in the model and also does not enter the following discussion, although a small inter-

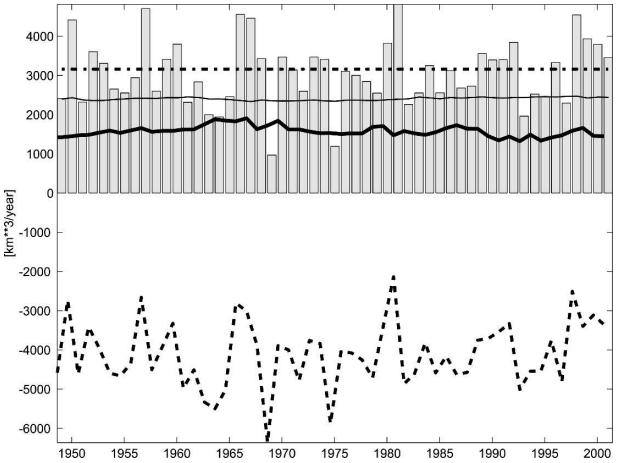

FIG. 5. Time series of the surface freshwater flux integrated over the Arctic as defined in Fig. 1. Integrated fluxes are given in kilometers cubed per year. The net flux (gray bars), the contribution by the net thermodynamic sea ice growth (dashed line), the constant flux adjustment (horizontal dash–dotted line), the $P - E$ (thick solid line), and the continental runoff (thin solid line) are shown.

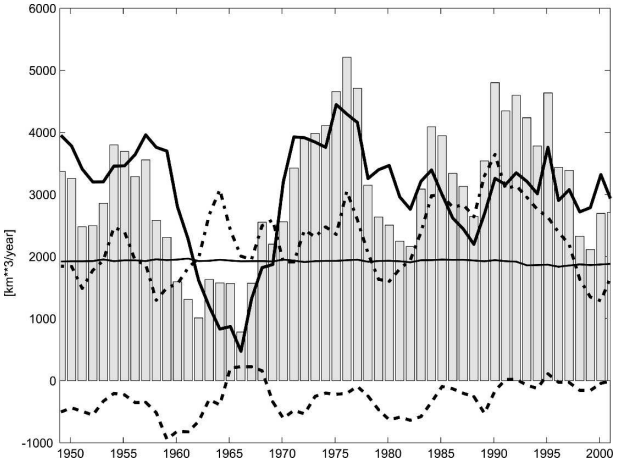

FIG. 6. Time series of the lateral freshwater fluxes out of the Arctic Ocean ($km^3\ yr^{-1}$). The total freshwater export (bars), the transport through Fram Strait (solid line), the transport through the Canadian Archipelago (dash–dotted line), the transport through the Barents Sea (dashed line), and the transport through Bering Strait (thin solid line) are shown.

annual variability is caused by variability in the local surface salinity that is used to transform the freshwater flux into an equivalent salt flux.

The lateral transports of liquid freshwater are dominated by the Fram Strait export. The Fram Strait freshwater export in turn is determined by the fresh southward component because the northward volume transport of Atlantic water is less than one-third of the East Greenland Current and the salinities of the inflow are much closer to the reference value than those of the outflow in the EGC. The Fram Strait export is responsible for the extremely low total export rates in the mid-1960s and for the large export of the mid-1970s.

The export through the Canadian Archipelago is somewhat smaller than the Fram Strait export and shows less variability. However, between the mid-1980s and the mid-1990s this component contributes significantly to the large freshwater exports during that period (Belkin et al. 1998). It is also largely responsible for overall decreasing exports after 1995. Because of the limited resolution of the model, the representation of the passage through the Canadian Archipelago is rather crude (Fig. 1). However, as we have shown in section 3b, the simulated mean freshwater transport through the Canadian Archipelago is within the range of recent observationally based estimates.

The total surface freshwater flux, its variability dominated by the thermodynamic ice growth and the corresponding brine release, freshwater export, and change of freshwater storage in the Arctic Ocean are displayed in Fig. 7. There is an apparent difference in the time scales of the variability in surface fluxes and export rate. The surface fluxes exhibit a much larger interannual variability, while the export rate is rather smoothly varying with a quasi-decadal time scale. On decadal to multidecadal time scales, the Arctic liquid freshwater reservoir thus responds mainly to changes in the export rate. The liquid freshwater export rate from the Arctic Ocean was extremely low in the 1960s and showed two periods of high values afterward. The late 1970s and early 1980s were especially characterized by large export rates. The high surface freshwater fluxes of 1966/67, 1983, and 1998 contributed to the peaks of freshwater content changes.

5. Mechanisms of freshwater content variability

a. Thermodynamic growth and ice export

Both Arctic freshwater reservoirs, the solid as well as the liquid, exhibit a decreasing trend since the end of the 1960s. KG03 found that the decline in Arctic sea ice volume between the 1960s and the 1990s was mainly due to a reduction in thermodynamic growth, while the sea ice export rate had no long-term trend except for the fact that thinner ice was reaching the straits leading to lower latitudes. The reduced brine release since 1970, or equivalently the higher freshwater flux into the ocean, owing to the trend in thermodynamic growth is also apparent in Fig. 7. Still, the total liquid freshwater content is decreasing over the same period because the increasing export rate is overcompensating the

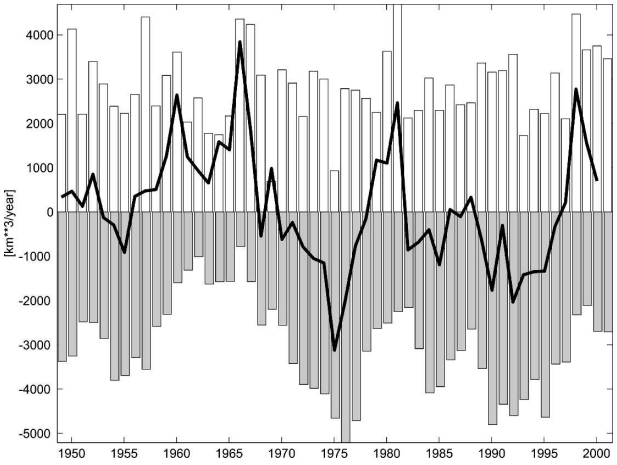

FIG. 7. Time series of the total surface freshwater fluxes (as in Fig. 5; positive bars) and the total lateral transports of freshwater (as in Fig. 6; negative bars). The solid line represents the rate of change of freshwater content in the Arctic Ocean. The total change in freshwater content is 4855 km^3 between the end and the start of the experiment, corresponding to an annual average imbalance of 78 $km^3\ yr^{-1}$ (see Table 2).

long-term reduced sea ice growth. The reduction in sea ice volume between maximum and minimum ice volume corresponds to a surface freshwater flux of 196 $km^3\ yr^{-1}$.

The brine release during sea ice formation is the largest surface forcing of freshwater content variability in the Arctic (Fig. 5). Arctic sea ice volume peaked in 1966, 1981, and 1988. The phases of sea ice growth correspond to relatively low surface freshwater fluxes for the ocean (Fig. 5). The ends of the ice accumulation phases are marked by relatively short episodes of enhanced freshwater flux to the ocean that contributed to large temporal rates of change in the liquid freshwater content. The enhanced freshwater flux is due to reduced sea ice production once the thickness has reached such large values that new ice production is hampered. These three episodes coincide with periods in which the liquid freshwater export was somewhat reduced so that both processes contributed to an increase in the liquid freshwater content.

b. Freshwater export after 1975

As shown above (Fig. 6), Fram Strait dominates the variability of the net liquid freshwater export from the Arctic in the model. We have calculated the quasi-northward (perpendicular to meridians of the rotated model grid) and quasi-southward components of all transports separately (not shown) and find that the quasi-southward component determines the Fram Strait transport variability. In the model, these volume transport fluctuations of the EGC are mostly compensated by northward flow through the Barents Sea.

The quasi-southward freshwater flux in Fram Strait is

$$\int_{\varphi_G}^{\varphi_S} a\, d\varphi \int_{-350\mathrm{m}}^{0\mathrm{m}} dz \left(v \frac{S - S_{\mathrm{ref}}}{S_{\mathrm{ref}}} \right),$$

with φ_G and φ_S the positions (latitudes in the rotated grid) of the Greenland and Svalbaard coasts, respectively, $S_{\mathrm{ref}} = 35$ psu, and $v \geq 0$ the velocity component perpendicular to the section. With temporal means and fluctuations $v = \langle v \rangle + v'$ and $S = \langle S \rangle + S'$ we break the transport down into three time-varying components (the part made up by $\langle v \rangle \langle S \rangle$ being constant in time) that are shown in Fig. 8a.

The variability of the southward freshwater transport in the Fram Strait is largely determined by the fluctuations in the volume transport (as expressed by the component $v' \langle S \rangle$), not by changes in the salinity of the Arctic ($\langle v \rangle S'$). The correlation of transport and salinity fluctuations only contributes somewhat to the reduction of the freshwater transport in the early 1960s. The volume transport has a pronounced minimum in the mid-1960s. It recovers until about 1975 when a rather smooth decline takes place until 1990.

Assuming negligible deep velocities, a simple 1.5-layer model (e.g., Vallis 2006, chapter 3.2) for the EGC yields a southward volume transport proportional to the square of the thickness of the active layer,

$$T_{\mathrm{EGC}} = -\int_{\varphi_G}^{\varphi_S} a\, d\varphi \int_{-h}^{0} v\, dz = \frac{g \Delta\rho}{2 \rho_o f} h_G^2.$$

Here $\Delta\rho$ is density depression of the active layer, g is the acceleration due to gravity, f is the Coriolis parameter, ρ_o is a reference density, and h is the thickness of the active layer. We assume that h vanishes somewhere between Greenland (where $h = h_G$) and Svalbaard. This transport estimate is shown in Fig. 8b with the position of the $S = 33.0$ psu surface taken as thickness of the Polar Water layer. The estimate agrees with the actual transport after 1975 (the correlation of the time series is 0.76), and the relationship between the Polar Water layer thickness and the volume transport can thus be used to discuss the fluctuations in the freshwater export during that period.

The correlations of the squared Polar Water layer thickness with various time series of potential forcing functions turned out to be insignificant. Neither the total liquid freshwater content of the Arctic Ocean nor atmospheric forcing as represented by simple indices like the SLP at the North Pole, the SLP difference across Fram Strait, or the NAO and the Arctic Oscil-

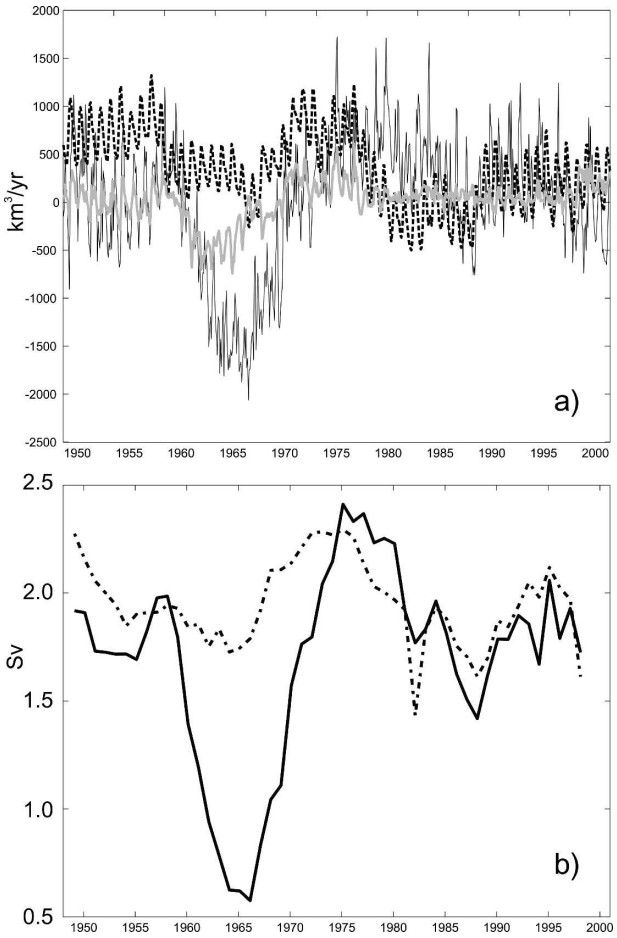

FIG. 8. (a) Time series of the components of the quasi-southward freshwater transport ($km^3\ yr^{-1}$) in Fram Strait as explained in the text. The gray line denotes the contribution by salinity fluctuation advected with the mean flow (area integral over $\langle v \rangle S'$), the solid black line indicates the contribution from fluctuating advection of mean salinity ($v'\langle S \rangle$), and the dashed black line shows the correlation of current and salinity anomalies ($v'S'$). All transports represent vertical integrals over all grid cells with quasi-southward mean flow. (b) The time series of the southward volume transport (Sv) in Fram Strait (solid) and the transport estimate using a simple 1.5-layer model (dash–dotted) are shown.

lation (AO) indices can explain much of the transport fluctuations after 1975.

Composite maps of Arctic freshwater content for years after 1975 with high and low (defined as one standard deviation above and below the mean) volume transport through Fram Strait (Fig. 9) show an Arctic-wide pattern. Positive volume transport anomalies are associated with enhanced freshwater content at the periphery (especially north of Greenland) and reduced freshwater content in the interior Arctic and the region affected by the Atlantic inflow. The anticyclonic Beaufort gyre diminishes in size and retreats eastward during phases of large freshwater export through Fram Strait. Associated with this retreat is a reorganization of the upper-layer flow field in the interior Arctic. The composites for high and low southward volume transport through Fram Strait show largest differences in the transpolar drift at 100-m depth (Fig. 9). The transpolar drift that carries most of the freshwater arriving at Fram Strait and the Canadian Archipelago generally splits into two branches in the model. One branch follows a rather straight path toward Fram Strait, while the other branch describes a cyclonic loop that first follows the northern extension of the Beaufort gyre before diverting into an eastward current that flows along the northern edges of the Canadian Archipelago and of Greenland toward Fram Strait. During a high-transport phase, this second branch is strengthened and relatively fresh water accumulates north of the Canadian Archipelago and Greenland. There might be a positive feedback as the convergence of relatively light water along the Greenland coast depresses the pycnocline, producing stronger geostrophic shear. The redistribution of freshwater from the interior of the Arctic Ocean to its periphery suggests fluctuations in Ekman transports as a possible cause for the thickness, and thus transport, fluctuations in Fram Strait. However, Ekman pumping integrated over the entire Arctic Ocean or over only the interior Arctic Ocean also does not yield a significant correlation with the transport in Fram Strait.

c. Extremely low freshwater export of the 1960s

The simple model fails for the extreme reduction of the freshwater export in the 1960s. During that period, large changes in the barotropic exchange through Fram Strait happened and the assumption of negligible lower-layer velocities is not valid. A comparison of the maps of the averaged streamfunction for the vertically integrated volume transport (not shown) for the periods 1960–65 (weak freshwater export) and 1975–80 (strong export) reveals that in the 1960s the Beaufort gyre was rather weak, while a strong cyclonic circulation cell existed in the Eurasian Basin. The latter had no apparent connection with the cyclonic cell of the Nordic seas, implying very low transports through Fram Strait. During the late 1970s, on the other hand, the cyclonic cell of the Nordic seas connects through the Barents Sea and Fram Strait with the Eurasian Basin cell.

Salinity in Fram Strait at a time of large freshwater export (Fig. 10b) is characterized by the fresh Polar Water in the west and the deep-reaching saline Atlantic water in the east. A strong front separates both water masses. In the early 1960s, on the other hand, there is

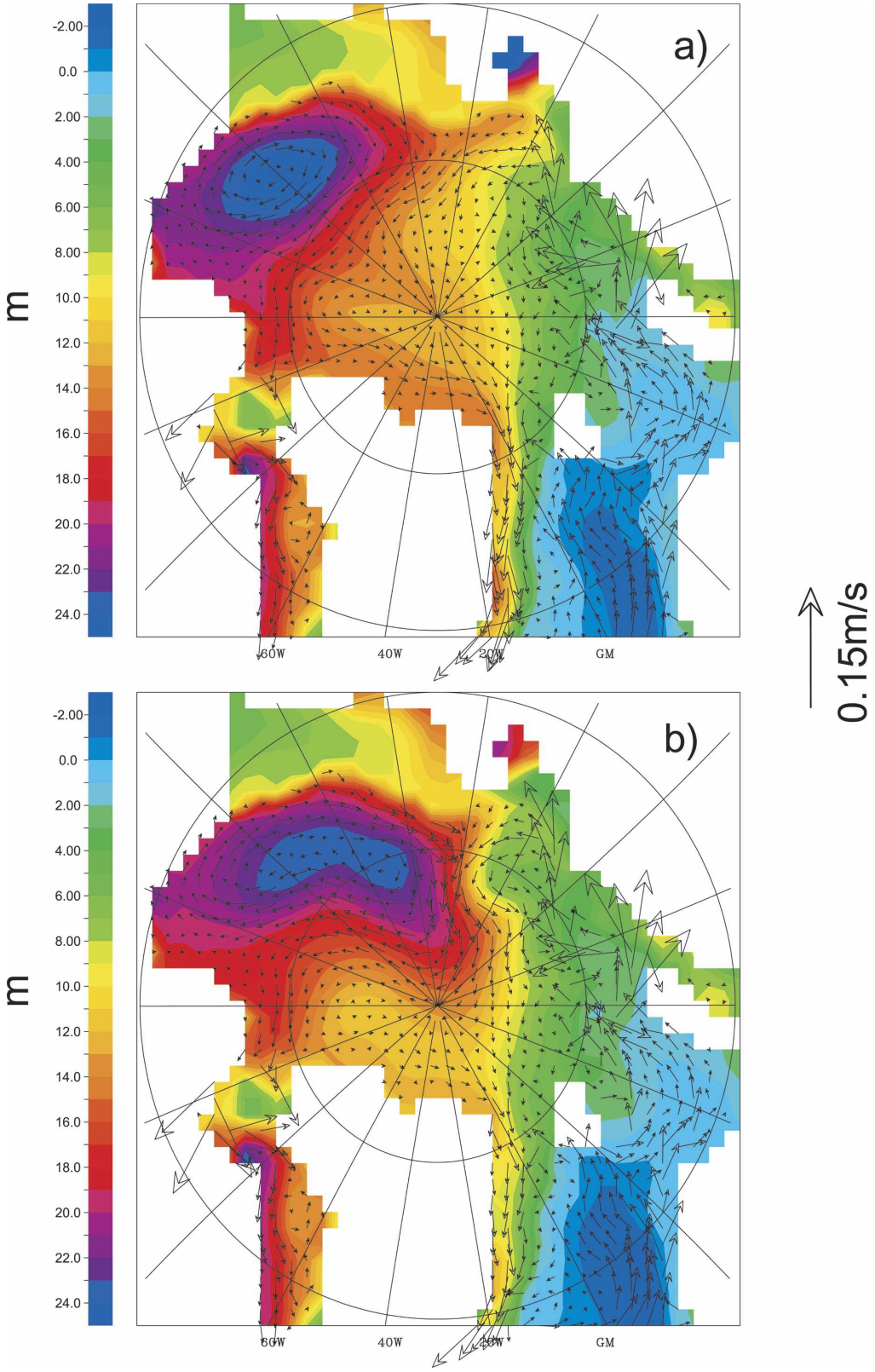

FIG. 9. Arctic freshwater content for the composites for (a) high (August 1974–July 1977, 1979–80, 1983–84, 1994–95) and (b) low (years August 1986–July 1989) southward volume transport through Fram Strait after 1975. Overlain are the corresponding velocity vectors at 100-m depth. A velocity scale is given on the right margin of the figure.

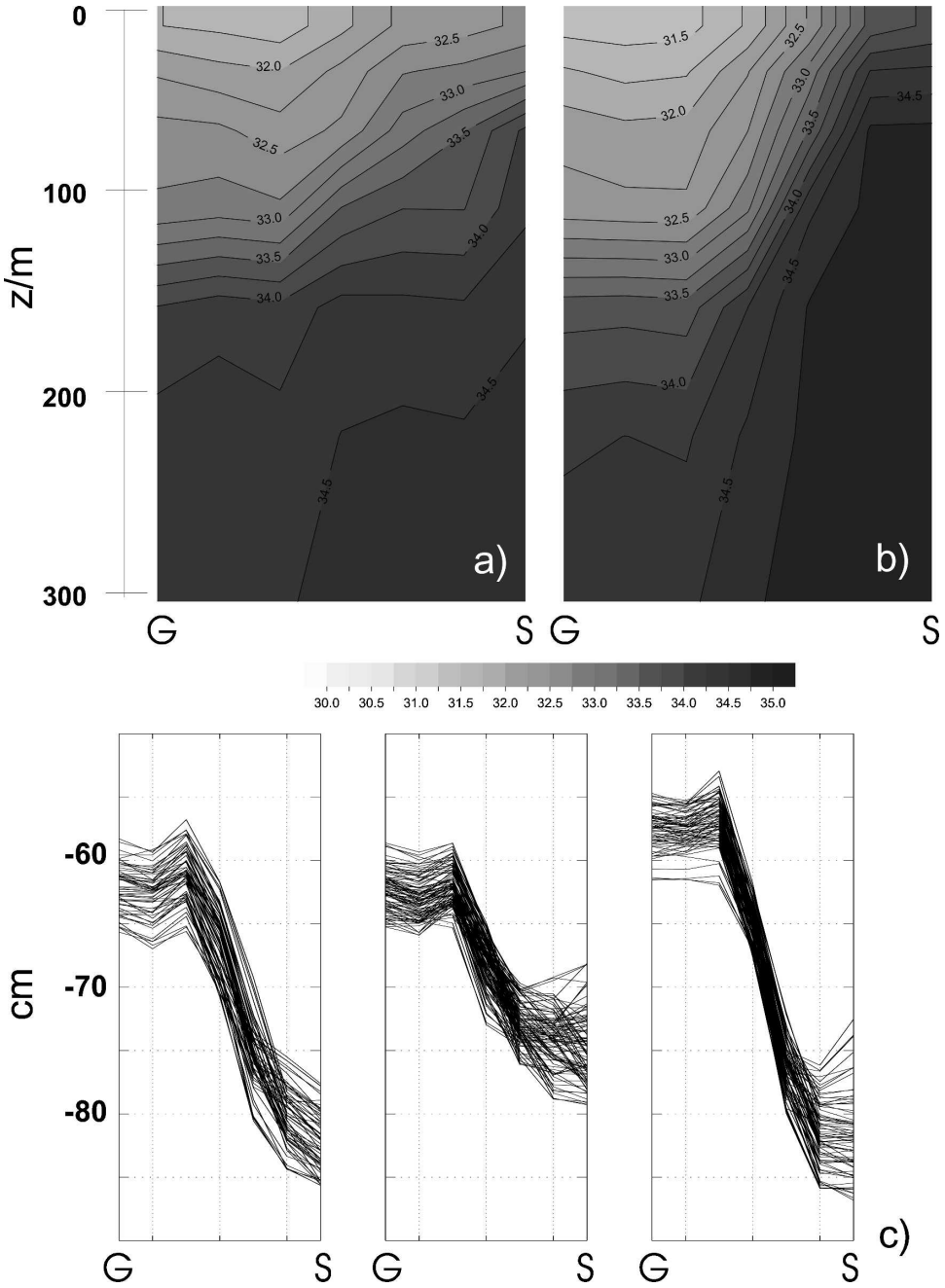

FIG. 10. Salinity section through Fram Strait (position see Fig. 1) averaged over (a) August 1964–July 1965 of low southward volume transport in the EGC and (b) August 1972–July 1973 of high transport in the EGC. Contour interval in both sections is 0.25 psu. (c) The steric height computed above 300 m for the years (left) 1955–59, (middle) 1960–67, and (right) 1968–75. Here G and S denote the Greenland and Svalbaard coasts, respectively.

little zonal salinity contrast in the upper 200 m (Fig. 10a). Low southward freshwater flow and anomalously low northward salt transport result in a strong reduction of the cross-strait density contrast and a strong reduction of the meridional exchange through the strait.

Reduced exchange through the strait implies that less saline Atlantic water enters the strait on its eastern side, and this positive feedback contributes to the persistence of the phenomena. The initial source of the freshwater in the West Spitzbergen Current (WSC), however, is an anomalous sea ice export from the Bar-

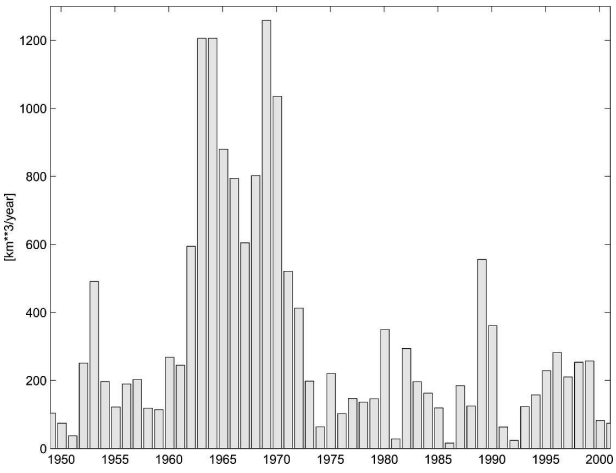

FIG. 11. Time series of net sea ice transport through a section between Svalbaard and Novaya Semlya (see Fig. 1). Positive values indicate southwestward transport. The mean transport over the duration of the simulation is 314 km^3 yr^{-1}.

ents Sea that feeds into the northward Norwegian–Atlantic Current. Analyzing Atlantic layer warming events, Gerdes et al. (2003) had identified an inflow of sea ice into the Barents Sea from the interior Arctic Ocean during the early 1960s. This inflow resulted in a very stable stratification and reduced heat loss from the ocean to the atmosphere. The time series of ice transport (Fig. 11) through a section from Svalbaard to the northern tip of Novaya Semlya shows southwestward ice transport in excess of 1000 km^3 yr^{-1} for several years in the early 1960s.

The long-term average transport rate across this line is only 314 km^3 yr^{-1}. The mean sea level difference after 1975 between the western and eastern margins of Fram Strait is 25 cm. During the low freshwater export event this difference dropped to 12 cm. The change is almost completely due to the change in salinity in the section; a recalculation of the steric height using climatological salinity revealed almost no change in surface elevation associated with the freshwater export minimum. In the early 1960s, the atmospheric sea level pressure field contains a high pressure anomaly that extends from around Iceland through the Nordic seas into the Eurasian Basin, implying anomalous ice drift of relatively thick interior Arctic origin sea ice into the northern Barents Sea (see Gerdes et al. 2003, their Fig. 4). Although this happened only once during our simulation period (Fig. 11), these conditions were similar to those that Kwok et al. (2005) have identified from satellite-tracked ice motion to be responsible for high sea ice transports from the Arctic interior to the Barents Sea in the winter 2002/03.

Referring to hindcast simulations with a sea ice model, Hilmer et al. (1998) describe the importance of the late-1960s ice transport through the Barents Sea for the generation of the Great Salinity Anomaly (GSA). The high ice transport into the Nordic seas was caused by an anomalously low SLP over the Kara and Laptev Seas and an anomalously high SLP north of the Canadian Archipelago and north of Iceland. They also show high ice transport from the Arctic proper into the Barents Sea in the early 1960s. This earlier maximum transport, occurring several years before the onset of the GSA, was associated with anomalously low ice export rates through Fram Strait. The later maximum transport enhanced the impact of the large ice export event through Fram Strait to result in the GSA. The sea ice transport results of Hilmer et al. (1998) are consistent with our results gained with a coupled ocean–sea ice model.

6. Discussion and conclusions

According to our hindcast simulation, the Arctic Ocean liquid freshwater balance over the last 50 years is governed by long-term fluctuations in the lateral exchanges with the subpolar North Atlantic. Surface fluxes vary predominantly on interannual time scale and are determined by the thermodynamic growth rate of sea ice in the Arctic. The freshwater content reached a maximum around 1965 and exhibited a decline to lowest values in the mid-1990s. The decline in the Arctic liquid freshwater content and the more or less coincident reduction in the Arctic sea ice volume (e.g., KG03) happened during the same time when the Nordic seas and the subpolar North Atlantic experienced rising freshwater content.

Curry and Mauritzen (2005) analyzed historical salinity data and showed an increase of the Nordic seas freshwater content by ~4000 km^3 and of the subpolar North Atlantic of ~15 000 km^3. These estimates nearly agree with the decrease in the Arctic freshwater reservoirs found in our simulation, suggesting a redistribution of freshwater between the Arctic and the Atlantic subpolar seas. Curry and Mauritzen point out that a large part of the subpolar freshening occurred between 1970 and 1975, that is, during the period when both sea ice export and liquid freshwater export through Fram Strait were large according to our simulation. Thus, our results suggest that a large part of the observed Atlantic subpolar freshening was caused by an anomalously large freshwater export from the Arctic. The contribution of the liquid freshwater was roughly 2 times that of the sea ice.

From the limited historic Arctic Ocean observations, Swift et al. (2005) deduced that the Arctic halocline and mixed layer became more saline in the mid-1970s and

then largely remained in that state. Consistent with Curry and Mauritzen (2005) they observe an increasing subpolar North Atlantic freshwater content during the same time, which suggests a redistribution of freshwater between the Arctic and the subpolar North Atlantic as a cause for both phenomena. Regarding the cause of the Arctic Ocean freshwater decline, Swift et al. dismiss changes in freshwater input and changes in Ekman pumping as possible causes. This is consistent with our simulation results and the conclusions of Häkkinen and Proshutinsky (2004). We find that changes in Ekman transport contributed to the redistribution of freshwater between the interior Arctic and its periphery and affected the Polar Water layer thickness in Fram Strait. However, Ekman pumping was not primarily responsible for the changes in total Arctic Ocean freshwater content.

According to our results, a freshwater content maximum in the mid-1960s Arctic Ocean was caused by extremely low freshwater export rates through Fram Strait (Fig. 6), caused by low volume transports in the EGC. Averaged from mid-1963 to mid-1969 the mean southward volume transport in the EGC was only 2.4 Sv; it increased to 4.0 Sv from mid-1975 to mid-1980. The inflow through Bering Strait is mostly balanced by the outflow through the Canadian Archipelago with a net value of about 1 Sv each. Consequently, the volume transport out of the Arctic through Fram Strait is balanced by the combined import in the West Spitzbergen Current and through the Barents Sea. Thus, the overall exchange between the Arctic and the Nordic seas was much reduced during the mid-1960s event.

The initial trigger of the Fram Strait volume transport anomaly in the 1960s was an anomalous sea ice export from the Barents Sea into the northward flowing Atlantic waters that determine the salinity of the WSC. A strong reduction in the zonal density gradient in Fram Strait resulted in a strong reduction in the sea surface height difference between Greenland and Svalbaard and a corresponding drop in the barotropic transport through the strait. The overall situation during the minimum export event is characterized by an anomalously high SLP over most of the Arctic Ocean and the Nordic seas. The anomalous atmospheric circulation favored ice transport from the interior Arctic Ocean through the Barents Sea to the Norwegian Sea. Stratification in the Barents Sea was enhanced, and heat losses over the Barents Sea reduced. The transport of Atlantic water into the Arctic Ocean through both pathways, Fram Strait and the Barents Sea, was reduced.

After the outstanding mid-1960s accumulation of freshwater in the Arctic, the Arctic freshwater content decreased until the mid-1990s. Only short periods of freshwater accumulation occurred in the early 1980s and during the last few years of the twentieth century. These episodes were supported by reduced sea ice production in the Arctic Ocean. After 1970, liquid freshwater export rates underwent fluctuations but were never again nearly as small as during most of the 1960s. An above-average export rate in the early 1970s can be explained by the large thickness of the Polar Water layer in Fram Strait and a correspondingly enhanced southward volume transport in the EGC. Since then, a downward trend in the southward liquid freshwater transport accompanies a decreasing Arctic liquid freshwater content. In this sense, the development of the Arctic liquid freshwater reservoir can be seen as an adjustment back toward long-term equilibrium conditions, driven by the feedback between liquid freshwater export and the thickness of the Arctic halocline. This adjustment occurs on a multidecadal time scale and might still be ongoing. This would imply a diminishing input of freshwater to the subpolar North Atlantic. However, stronger sources (Peterson et al. 2002; Wu et al. 2005) will probably increase the thickness of the Arctic halocline and subsequently the liquid freshwater export through Fram Strait in the future. The development during the last three to four decades cannot be taken as a part of the response of the Arctic Ocean to human-induced changes of the climate system. It rather appears as the slow adjustment after a rapid increase in Arctic liquid freshwater content caused by a coincidence of rare events forced by an anomalous atmospheric circulation that lasted for several years in the 1960s.

Acknowledgments. NCEP–NCAR reanalysis data were provided by the NOAA–CIRES Climate Diagnostics Center, Boulder, Colorado, from their Web site (online at http://www.cdc.nooa.gov). We thank Christian Dieterich for providing boundary values from the FLAME model of Kiel University. This work was partly funded by the DEKLIM project (BMBF Contract 01 LD 0047) and the SFB 512 "Low pressure systems and the climate system of the North Atlantic" of the DFG. Further contributions came from INTAS "Nordic seas in the global climate system" (INTAS Reference Number 03-51-4260) and the Arctic Ocean Model Intercomparison Project (AOMIP).

REFERENCES

Aagaard, K., and E. C. Carmack, 1989: The role of sea ice and other fresh water in the Arctic circulation. *J. Geophys. Res.,* **94,** 14 485–14 498.

Belkin, I. M., S. Levitus, J. Antonov, and S.-A. Malmberg, 1998: "Great Salinity Anomalies" in the North Atlantic. *Progress in Oceanography,* Vol. 41, Pergamon, 1–68.

Carmack, E., 2000: The Arctic Ocean's freshwater budget: Sources, storage and export. *Freshwater Budget of the Arctic Ocean,* E. L. Lewis, Ed., Kluwer Academic, 91–126.

Curry, R., and C. Mauritzen, 2005: Dilution of the northern North Atlantic Ocean in recent decades. *Science,* **308,** 1772–1774.

Dickson, R. R., J. Meincke, S.-A. Malmberg, and A. J. Lee, 1988: The "Great Salinity Anomaly" in the northern North Atlantic 1968–1982. *Progress in Oceanography,* Vol. 20, Pergamon, 103–151.

——, I. Yashayaev, J. Meincke, B. Turrell, S. Dye, and J. Holfort, 2002: Rapid freshening of the deep North Atlantic Ocean over the past four decades. *Nature,* **416,** 832–837.

Gerdes, R., and U. Schauer, 1997: Large scale circulation and water mass distribution in the Arctic Ocean from model results and observations. *J. Geophys. Res.,* **102,** 8467–8483.

——, C. Köberle, and J. Willebrand, 1991: The influence of numerical advection schemes on the results of ocean general circulation models. *Climate Dyn.,* **5,** 211–226.

——, M. J. Karcher, F. Kauker, and U. Schauer, 2003: Causes and development of repeated Arctic Ocean warming events. *Geophys. Res. Lett.,* **30,** 1980, doi:10.1029/2003GL018080.

Griffies, S. M., and Coauthors, 2005: Formulation of an ocean model for global climate simulations. *Ocean Sci.,* **1,** 45–79.

Häkkinen, S., and A. Proshutinsky, 2004: Freshwater content variability in the Arctic Ocean. *J. Geophys. Res.,* **109,** C03051, doi:10.1029/2003JC001940.

Hansen, B., W. R. Turrell, and S. Østerhus, 2001: Decreasing overflow from the Nordic seas into the Atlantic Ocean through the Faroe Bank channel since 1950. *Nature,* **411,** 927–930.

Harder, M., 1996: Rauhigkeit und Alter des Meereises in der Arktis—Numerische Untersuchungen mit einem großskaligen Modell (in German with English summary). Ph.D. thesis, Alfred-Wegener-Institut, Berichte zur Polarforschung No. 203, 127 pp.

Hibler, W. D., 1979: A dynamic thermodynamic sea ice model. *J. Phys. Oceanogr.,* **9,** 815–846.

——, and K. Bryan, 1987: A diagnostic ice-ocean model. *J. Phys. Oceanogr.,* **17,** 987–1015.

Hilmer, M., 2001: A model study of Arctic Sea ice variability. Ph.D. thesis, Institut für Meereskunde an der Universität Kiel, Berichte aus dem Institut für Meereskunde No. 320, 157 pp.

——, M. Harder, and P. Lemke, 1998: Sea ice transport: A highly variable link between Arctic and North Atlantic. *Geophys. Res. Lett.,* **25,** 3359–3362.

Holloway, G., and T. Sou, 2002: Has Arctic sea ice rapidly thinned? *J. Climate,* **15,** 1691–1701.

Köberle, C., and R. Gerdes, 2003: Mechanisms determining the variability of Arctic sea ice conditions and export. *J. Climate,* **16,** 2843–2858.

Kreyscher, M., M. Harder, P. Lemke, and G. M. Flato, 2000: Results of the Sea Ice Model Intercomparison Project: Evolution of sea ice rheology schemes for use in climate simulations. *J. Geophys. Res.,* **105,** 11 299–11 320.

Kwok, R., W. Maslowski, and S. W. Laxon, 2005: On large outflows of Arctic sea ice into the Barents Sea. *Geophys. Res. Lett.,* **32,** L22503, doi:10.1029/2005GL024485.

Lemke, P., W. D. Hibler, G. Flato, M. Harder, and M. Kreyscher, 1997: On the improvement of sea ice models for climate simulations: The Sea Ice Model Intercomparison Project. *Ann. Glaciol.,* **25,** 183–187.

Lohmann, G., R. Gerdes, and D. Chen, 1996: Sensitivity of the thermohaline circulation in coupled oceanic GCM–atmospheric EBM experiments. *Climate Dyn.,* **12,** 403–416.

Mauritzen, C., 1996: Production of dense overflow waters feeding the North Atlantic across the Greenland-Scotland Ridge. Part 1: Evidence for a revised circulation scheme. *Deep-Sea Res. I,* **43,** 769–806.

Melling, H., 2000: Exchanges of freshwater through the shallow straits of the North American Arctic. *Freshwater Budget of the Arctic Ocean,* E. L. Lewis, Ed., Kluwer Academic, 479–502.

Meredith, M. P., K. J. Heywood, P. F. Dennis, L. E. Goldson, R. M. P. White, E. Fahrbach, U. Schauer, and S. Østerhus, 2001: Freshwater fluxes through the western Fram Strait. *Geophys. Res. Lett.,* **28,** 1615–1618.

National Geophysical Data Center, 1988: Digital relief of the surface of the earth. ETOPO5 data, NOAA Data Announcement 88-M66-02.

Pacanowski, R. C., 1995: MOM 2 documentation, user's guide and reference manual. Geophysical Fluid Dynamics Laboratory/Princeton University Ocean Group Tech. Rep. 3, 232 pp.

Parkinson, C. L., and W. M. Washington, 1979: A large scale numerical model of sea ice. *J. Geophys. Res.,* **84,** 311–337.

Peterson, B. J., R. M. Holmes, J. W. McClelland, C. J. Vörösmarty, R. B. Lammers, A. I. Shiklomanov, I. A. Shiklomanov, and S. Rahmstorf, 2002: Increasing river discharge to the Arctic Ocean. *Science,* **298,** 2171–2173.

Prange, M., and R. Gerdes, 2006: The role of surface freshwater flux boundary conditions in Arctic Ocean modeling. *Ocean Modell.,* **13,** 25–43.

Prinsenberg, S. J., and J. Hamilton, 2004: The oceanic fluxes through Lancaster Sound of the Canadian Arctic Archipelago. *ASOF Newsletter,* Vol. 2, 8–11.

Rahmstorf, S., and J. Willebrand, 1995: The role of temperature feedback in stabilizing the thermohaline circulation. *J. Phys. Oceanogr.,* **25,** 787–805.

Roach, A. T., K. Aagaard, C. H. Pease, S. A. Salo, T. Weingartner, V. Pavlov, and M. Kulakov, 1995: Direct measurements of transport and water properties through the Bering Strait. *J. Geophys. Res.,* **100,** 18 443–18 457.

Röske, F., 2006: A global heat and freshwater forcing data set for ocean models. *Ocean Modell.,* **11,** 235–297.

Rothrock, D. A., Y. Yu, and G. A. Maykut, 1999: Thinning of the Arctic sea-ice cover. *Geophys. Res. Lett.,* **26,** 3469–3472.

Shiklomanov, I. A., A. I. Shiklomanov, R. B. Lammers, B. J. Peterson, and C. J. Vorosmarty, 2000: The dynamics of river water inflow to the Arctic Ocean. *Freshwater Budget of the Arctic Ocean,* E. L. Lewis, Ed., Kluwer Academic, 281–296.

Steele, M., and T. Boyd, 1998: Retreat of the cold halocline layer in the Arctic Ocean. *J. Geophys. Res.,* **103,** 10 419–10 435.

——, D. Thomas, and D. A. Rothrock, 1996: A simple model study of the Arctic freshwater balance, 1979–1985. *J. Geophys. Res.,* **101,** 20 833–20 848.

——, R. Morley, and W. Ermold, 2001a: PHC: Global ocean hydrography with a high quality Arctic Ocean. *J. Climate,* **14,** 2079–2087.

——, and Coauthors, 2001b: Adrift in the Beaufort Gyre: A model intercomparison. *Geophys. Res. Lett.,* **28,** 2935–2938.

Stevens, D. P., 1991: The open boundary condition in the United Kingdom fine-resolution Antarctic model. *J. Phys. Oceanogr.,* **21,** 1494–1499.

Swift, J. H., K. Aagaard, L. Timokhov, and E. G. Nikiforov, 2005: Long-term variability of Arctic Ocean waters: Evidence from a reanalysis of the EWG data set. *J. Geophys. Res.,* **110,** C03012, doi:10.1029/2004JC002312.

Timokhov, L., and F. Tanis, Eds., 1997: *Environmental Working Group Joint U.S.–Russian Atlas of the Arctic Ocean—Winter Period*. Environmental Research Institute of Michigan in association with the National Snow and Ice Data Center, Arctic Climatology Project CD-ROM.

——, and ——, Eds., 1998: *Environmental Working Group Joint U.S.–Russian Atlas of the Arctic Ocean—Summer Period*. Environmental Research Institute of Michigan in association with the National Snow and Ice Data Center, Arctic Climatology Project CD-ROM.

Tucker, W. B., J. M. Weatherly, D. T. Eppler, and L. D. Farmer, 2001: Evidence for rapid thinning of sea ice in the western Arctic Ocean at the end of the 1980s. *Geophys. Res. Lett.,* **28,** 2851–2854.

Vallis, G. K., 2006: *Atmospheric and Oceanic Fluid Dynamics*. Cambridge University Press, 745 pp.

Vinje, T., 2001: Fram Strait ice fluxes and atmospheric circulation, 1950–2000. *J. Climate,* **14,** 3508–3517.

Wadhams, P., and N. R. Davis, 2000: Further evidence of ice thinning in the Arctic Ocean. *Geophys. Res. Lett.,* **27,** 3973–3975.

Woodgate, R. A., and K. Aagaard, 2005: Revising the Bering Strait freshwater flux into the Arctic Ocean. *Geophys. Res. Lett.,* **32,** L02602, doi:10.1029/2004GL021747.

Wu, P., R. Wood, and P. Stott, 2005: Human influence on increasing Arctic river discharges. *Geophys. Res. Lett.,* **32,** L02703, doi:10.1029/2004GL021570.

Xie, P. P., and P. A. Arkin, 1996: Analyses of global monthly precipitation using gauge observations, satellite estimates, and numerical model predictions. *J. Climate,* **9,** 840–858.

Zalesak, S. T., 1979: Fully multidimensional flux-corrected transport algorithms for fluids. *J. Comput. Phys.,* **31,** 335–362.

Zhang, J., D. Rothrock, and M. Steele, 2000: Recent changes in Arctic sea ice: The interplay between ice dynamics and thermodynamics. *J. Climate,* **13,** 3099–3114.

Zhang, S., R. J. Greatbatch, and C. A. Lin, 1993: A reexamination of the polar halocline catastrophe and implications for coupled ocean–atmosphere modeling. *J. Phys. Oceanogr.,* **23,** 287–299.